Presenilin-1–associated abnormalities in regional cerebral perfusion

K. A. Johnson [3,4] **MD**
F. Lopera [1] **MD**
K. Jones [2] **PhD**
A. Becker [3] **BS**
R. Sperling [3] **MD**
J. Hilson [3] **BS**
J. Londono [1] **MD**
I. Siegert [1] **MD**
M. Arcos [1] **PhD**
S. Moreno [1] **MA**
L. Madrigal [1] **RN**
J. Ossa [1] **PhD**
N. Pineda [1] **MD**
A. Ardila [1] **MD**
M. Roselli [1] **PhD**
M. S. Albert [4] **PhD**
K. S. Kosik [3] **PhD**
A. Rios [1] **MD**

[1] Antioquia University School of Medicine Colombia (Drs. Lopera, Londono, Siegert, Arcos, Ossa, Pineda, Ardila, Roselli, and Rios, and S. Moreno and L. Madrigal)Medellin
[2] Brandeis University (Dr. Jones)Waltham
[3] Brigham and Women's Hospital (Drs. Johnson, Sperling, and Kosik, and A. Becker and J. Hilson
[4] Massachusetts General Hospital (Drs. Johnson and Albert), Harvard Medical SchoolBoston, MA.

Article abstract—

Objective: **To investigate the influence of the presenilin-1 gene (*PS-1*) mutation on regional cerebral perfusion, SPECT was evaluated in 57 individuals. The subjects were members of a large pedigree from Colombia, South America, many of whom carry a *PS-1* mutation for early-onset AD. *Methods:* Members of this large kindred who were cognitively normal and did not carry the *PS-1* mutation (n = 23) were compared with subjects who were carriers of the mutation but were asymptomatic (n = 18) and with individuals with the mutation and a clinical diagnosis of AD (n = 16). Cerebral perfusion was measured in each subject using hexamethylpropyleneamine oxime SPECT. The data were analyzed in two ways: 1) Mean cerebral perfusion in each of 4320 voxels in the brain was compared among the groups using *t*-tests (*t*-maps); and 2) each individual received a weighted score on 20 vectors (factors), based on a large normative sample (n = 200), using a method known as singular value decomposition (SVD). *Results:* Based on *t*-maps,**

subjects with the *PS-1* mutation who were asymptomatic demonstrated reduced perfusion in comparison with the normal control subjects in the hippocampal complex, anterior and posterior cingulate, posterior parietal lobe, and anterior frontal lobe. The AD patients demonstrated decreased perfusion in the posterior parietal and superior frontal cortex in comparison with the normal control subjects. Discriminant function analysis of the vector scores derived from SVD (adjusted for age and gender) accurately discriminated 86% of the subjects in the three groups ($p < 0.0005$). *Conclusion:* Regional cerebral perfusion abnormalities based on SPECT are detectable before development of the clinical symptoms of AD in carriers of the *PS-1* mutation.

Supported by National Institute on Aging (P01-AG04953) and by the Colciencias Project of Colombia (1115-04-040-95 and 115-04-409-98).
Received August 23, 2000.
Accepted in final form February 8, 2001.

Address correspondence and reprint requests to Dr. Keith A. Johnson, Radiology and Neurology, Brigham and Women's Hospital, Harvard Medical School, 75 Francis St., Boston, MA 02115; e-mail: keith@bwh.harvard.edu

The majority of patients with AD under the age of 60 carry a mutation in the presenilin-1 gene (*PS-1*). At least 50 such mutations on the *PS-1* gene have been identified among over 80 families of various ethnic origins.[1] These mutations confer autosomal dominant inheritance, with virtually 100% penetrance. One of these mutations, which occurs at codon 280 in the *PS-1* gene, has been identified in a large multigenerational family living in Colombia, South America.[2] Individuals with this mutation will therefore eventually develop AD, if they live through the age of risk, whether or not they are symptomatic at any one point in time. The average age at onset of AD in this kindred is 47 years.

A number of MR studies have been conducted in pedigrees with a *PS-1* mutation.[3] However, to our knowledge, there have been no studies of cerebral perfusion in individuals with mutations of the *PS-1* gene.

Several studies of glucose metabolism have, however, been conducted in subjects with the one widely agreed upon genetic risk factor for late-onset AD, the ε4 allele of the *APOE* gene. The ε4 allele of the *APOE* gene is associated with an increased risk for AD and modifies age at onset,[4] but it does not act as a dominant, fully penetrant gene. Reiman et al.,[5] using PET, examined subjects who were homozygous for the *APOE-4* allele but did not demonstrate evidence of memory problems. This group of asymptomatic at-risk subjects demonstrated decreased metabolism in temporoparietal cortical regions. These investigators also found perfusion decreases in the posterior cingulate and prefrontal cortex. Small et al. examined subjects with mild memory problems who were *APOE-4* positive and had a family history of AD.[6] Using PET, they found decreased parietal metabolism in the *APOE-4* carriers. These perfusion decreases reported in *APOE-4* carriers are consistent with functional imaging studies in established cases of AD, the majority of whom have demonstrated prominent abnormalities in the association cortices of the temporal and parietal cortex.[7] [8] [9] [10] [11] [12]

The frequency of such decreases is increasingly common as the severity of disease increases[13] [14] [15] and is related to the underlying burden of pathology.[16]

We sought to determine whether a pattern of abnormal cerebral perfusion could be identified in *PS-1* carriers who were asymptomatic. To address this issue, SPECT was evaluated in 57 individuals who were members of a large pedigree from Colombia, South America, many of whom carry the *PS-1* mutation for AD. Based on a previous SPECT study in subjects with preclinical AD[17] and the PET studies cited above, we hypothesized that regional perfusion decreases would occur in the hippocampal–amygdaloid region and the cingulate gyrus in the asymptomatic individuals with the *PS-1* mutation. Based on the extensive literature in cases with established AD, we hypothesized that temporoparietal decreases in perfusion would characterize the individuals with clinical evidence of AD caused by a *PS-1* mutation.

Methods.

Subjects.

Participants in the study consisted of 57 subjects from a large extended family living in Colombia, South America, many of whom carry a *PS-1* mutation for early-onset AD at codon 280. This population was divided into three subgroups: Group 1 (normal control subjects) consisted of 23 individuals (8 men, 15 women) who were cognitively normal and did not carry the *PS-1* mutation. Their mean score on the Spanish version of the Mini-Mental State Examination (MMSE)[18] was 28.2. They had a mean age of 42.7 ± 7.9. Group 2 (asymptomatic carriers) consisted of 18 individuals (9 men and 9 women) who were carriers of the mutation but were asymptomatic; their mean MMSE score was 27.7. The mean age of this group was 38.1 ± 7.2 years. Group 3 (patients with AD) consisted of 16 individuals (6 men and 10 women) who carried the *PS-1* mutation and met the criteria for a clinical research diagnosis of probable AD[19] ; their mean MMSE score was 12. They had a mean age of 51.0 ± 6.4 years.

The mean MMSE scores for Groups 1 and 2 were not significantly different from one another. The mean age of Group 1 did not differ from that of Group 3. Group 3 was, however, significantly older than Group 2 ($p < 0.01$), and the difference between the ages of Groups 1 and 2 approached significance ($p < 0.06$).

In addition, a large number of control subjects were used as a normative sample for the purpose of calculating some of the SPECT data presented here. Analyses employing this sample have been previously published.[17] [20] The characteristics of the normative sample and the Colombian kindred are described below.

Subjects from the Colombian kindred.

Five pedigrees from Antioquia, Colombia, with an index case of early-onset AD, were identified as previously reported.[2] From this population, a sample of 82 individuals were recruited by directly contacting subjects who lived relatively close to the imaging facility (i.e., Angostura, Yarumal, Santa Rosa de Osos, Ituango, San Jose de la Montana, Dadeiba, Sopetran, Cedeno, Sabanalarga, Medellin, and Belmira). Each

subject (or family member, if necessary) gave informed consent, according to a protocol approved by the Human Subjects Committee of the University of Antioquia.

All subjects received a medical, neurologic, and neuropsychologic examination to determine whether or not they met National Institute of Neurologic, Communicative Disorders and Stroke/AD and Related Disorders criteria.[19] The medical examination included standard laboratory tests (e.g., serum chemistry and hematology, thyroid and liver function tests, and brain MRI). The neuropsychological testing employed the Spanish version of the following tests: a test battery developed by the Consortium to Establish a Registry for AD,[21] the Boston Naming Test, [22] the Boston Diagnostic Aphasia Examination, [23] and the Rey–Osterreith Complex Figure. [24] Additional nonstandardized neuropsychological tests were included for research purposes. In addition, blood was collected to determine the presence of the *PS-1* mutation. The subjects who were classified as asymptomatic were active and functionally normal and had no significant cognitive complaints and no evidence of cognitive impairments, based on the standardized neuropsychological tests. Of the 81 participants, 19 were excluded from further study because they had a variety of reasons for the cognitive deficits and did not meet criteria for AD. To obtain comparable ages for the normal control subjects and the asymptomatic carriers, five asymptomatic carriers were excluded from the analyses.

Control subjects used for development of SPECT vectors.

One of the SPECT analysis procedures described below employs a procedure known as singular value decomposition (SVD), which is comparable with a factor analysis and requires a large group of normal control subjects to generate stable parameters. Vector scores (similar to factor scores) are then generated for each individual. These scores reflect the degree to which that subject's regional brain perfusion compares with those of normal individuals. The subjects used to establish the “normal” profile for the SPECT vectors consisted of 200 individuals from the greater Boston area who were considered to be normal on the basis of a lengthy screening process.[20] Volunteers were recruited primarily through the print media and were first screened by a telephone interview. Subjects with a history of significant head trauma, neurologic or psychiatric illness, major medical disease, or use of medication with psychoactive properties (including certain classes of antihypertensives) were excluded. Subjects with mild medical conditions such as osteoporosis or arthritis were included. Approximately half of the control subjects were recruited through the Massachusetts Institute of Technology Clinical Research Center and half were recruited through the Gerontology Research Unit of Massachusetts General Hospital. All subjects considered appropriate for further evaluation received a physical, neurologic, and psychiatric assessment. In addition, an EKG was performed, and blood and urine specimens were analyzed to rule out evidence of occult disease (e.g., urinalysis, complete blood count, etc). Any subject found to have a clinically significant abnormality on the basis of this evaluation was excluded. The potential participants were also administered a series of standardized cognitive tests to identify subjects with evidence of cognitive impairment. These included the vocabulary subtest of the Wechsler Adult Intelligence Scale–revised,[25] the Logical Memory Subtest of the Wechsler Memory Scale,[26] the Rey–Osterreith Complex Figure Test,[24] and the MMSE.[18] Any subjects with scores on these tests that fell outside the normal range were eliminated. Each of these 200 individuals was studied with perfusion SPECT as part of the evaluation. A detailed description of the SPECT data from this sample has been

previously presented.[20] These control values were used for the vector analysis only. The *t*-map procedure described below employed SPECT data obtained only from members of the *PS-1* kindred in Colombia.

SPECT acquisition.

Subjects in the sample from the Colombian kindred (n = 57) underwent imaging using a rotating gamma camera (Sopha model DSX, Sopha Medical Systems, Columbia, MD), equipped with a low-energy, high-resolution collimator. The measured resolution was 10.0 mm. Subjects in the normative sample (n = 200) underwent imaging using a digital dedicated brain-imaging system (Cerespect; Digital Scintigraphics, Waltham, MA) consisting of a stationary annular NaI crystal and rotating collimator system.[27] The measured resolution, using capillary line sources, was 7.3 mm at 9 mm from center for ^{99m} Tc.[28]

All subjects in both samples were scanned 20 minutes after injection of 20.0 ± 1.0 mCi of ^{99m} Tc-hexamethylpropyleneamine oxime (Ceretec, Amersham, UK) with the subjects supine at rest, with eyes open, in a darkened room, with ambient white noise. Total acquisition times were ≈ 30 minutes. Datasets were corrected for scatter and attenuation, reconstructed using filtered back-projection, transferred by network for further processing, and displayed as a set of 64 slices (1.67-mm slice thickness) using a 128 ×128 matrix (167 × 1.67 × 2-mm pixels).

Anatomic orientation, surface contouring, and scaling procedures for the SPECT data were performed as detailed previously.[12] In brief, each dataset was oriented to a set of spatial reference standards, based on a modification of a standard atlas.[29] The topmost slice representing activity from the thalamus was defined as a reference slice, and 10 slices (thickness = 5 ×1.67 mm = 8.54 mm) were defined above and below the reference slice. Individual surface contouring accomplished scaling in *x* and *y* planes. To reduce individual differences in perfusion that might be related to brain atrophy, the image processing included a volume-scaling procedure. This procedure, which uses brain surface contours,[12] scales smaller brains and brains with larger sulci to a standard space. This reduces artifactual count density reductions due to enlarged sulci near the brain surface. It does not eliminate artifacts arising from deeper, enlarged sulci or from enlarged ventricles. Thus, it reduces, but does not completely eliminate, the effects of atrophy.

A polar grid, consisting of spokes and contours that are concentric with and the same shape as the external contour, was then superimposed on each slice. Forty-eight radial spokes and nine bands were generated for each dataset, forming 432 “macrovoxels” per slice and over 10 slices 4320 macrovoxels per dataset. Cerebral perfusion was measured using an automated algorithm yielding mean count density (counts/voxel) within each of 4320 macrovoxels in each subject. Count densities were then normalized to remove the effects of global perfusion.[12] This normalization procedure uses the part correlation coefficient between each individual's adjusted macrovoxel and the dependent variable (i.e., in this case, group membership). The adjustment of the macrovoxel uses the individual's global perfusion and a weight derived from the correlation between that macrovoxel and the global perfusion across the group. When this part correlation coefficient is converted to a *t* value, it is identical to the covariance adjustment employed in statistical parametric mapping (SPM).[30] [31] [32]

Data analysis.

The normalized count density measures within each of the 4320 macrovoxels were then analyzed in two ways[1] : application of the *t*-statistic to each macrovoxel, in a manner similar to SPM and application of SVD to the macrovoxel data.

T-map analysis.

In the *t*-map analysis, Student's *t*-statistic was applied to normalized count density measures within each macrovoxel and Groups 1 to 3 were compared pairwise. Each macrovoxel that had a *t* value of ±4 ($p < 0.00005$, one-sided) was visually displayed according to a pseudo-color scale, as described below. This method is similar to the SPM technique commonly used in the analysis of PET data.[31] [33] Groups 1 to 3 were compared pairwise, as follows: normal control noncarriers versus AD patient carriers, normal control noncarriers versus asymptomatic carriers, and asymptomatic carriers versus AD patient carriers.

Vector score analysis.

In the method based on SVD, 20 weighted scores were calculated for each subject, based on 20 vectors derived from the normative sample described above (n = 200), using a method previously described.[17] [20] In brief, the normative group was used to compute the weighting coefficients for 20 vectors, which together represent the normal pattern of brain activity covariance. These vector scores were then entered into a set of discriminant function analyses to determine the degree to which the groups could be discriminated.

Visual display and evaluation of the data.

To relate the perfusion data produced by the *t*-map analysis to its underlying anatomy, an iterative surface-matching algorithm was used to generate a rigid body transformation. The data were then superimposed on a composite MR image based on 305 subjects.[34] This composite MR image was scaled to the Talairach coordinate system.[29] The superimposed images were then examined to determine the brain regions that contributed to the discrimination between the groups. Positive *t* values that exceeded an a priori significance level (±4) were shown in shades of red and negative values were shown in shades of blue. Brain regions were labeled based on those that produced activation in eight or more contiguous size-averaged voxels. Talairach coordinates were then provided for each region. Thus, the SPECT data were used to display the macrovoxels throughout the brain in terms of the differences among the groups, and the regions contributing to the difference were identified. It should be emphasized that this “back-projection” was not itself a method of discriminating the groups but rather a method of portraying the group differences that had been established by *t*-test.

Correlation between SPECT data and neuropsychological test scores.

The SPECT vector scores, described above, were correlated with performance on the neuropsychological test battery to determine whether there was a relationship between SPECT perfusion and performance on the tests.

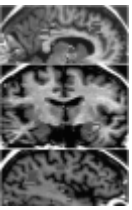

Results.

T-map analysis.

A *t*-map was generated for each of the three pairwise comparisons. The results were as follows:

1. Normal control noncarriers versus asymptomatic carriers. Of the 4320 macrovoxels examined, 267 had decreased perfusion in the asymptomatic carriers compared with the normal controls. Regions with greatest reductions included the anterior cingulate bilaterally and the right posterior cingulate (figure 1 A), the hippocampal complex on the left (figure 1 B), and the temporoparietal cortex (figure 1 C). The table provides the Talairach coordinates for the regions with reduced perfusion in this comparison and in those described below.
2. Normal control noncarriers versus AD patients. Of the 4320 macrovoxels examined, 1079 had reduced perfusion in the AD patients in comparison with the normal control noncarriers. Regions with greatest reductions were seen in the temporoparietal cortex bilaterally (figure 2A). The patients with AD also differed from the normal control noncarriers in the regions identified in figure 1 .
3. Asymptomatic carriers versus AD patients. Of the 4320 macrovoxels examined, 639 had decreased perfusion in the AD patients compared with the asymptomatic carriers. Regions with the greatest reductions were found in the temporoparietal cortex bilaterally (figure 2B). The asymptomatic carriers also differed from the AD patients in the regions identified in figure 1 .

Figure 1. *This figure represents the regions (shown in color) in the anterior and posterior cingulate (A), hippocampal–amygdaloid complex (B), and temporoparietal cortex (C) that significantly differentiated the normal control noncarriers from the asymptomatic presenilin-1 gene mutation carriers. The SPECT data are overlaid on a typical MR image in sagittal section. The anatomic labels assigned to the regions are based on the examination of the t-map overlay on an average MR image obtained from 152 individuals.*[34] *The data were scaled to the Talairach coordinate system. The significant differences between the groups are highest within the region that is at the red end of the spectrum and lowest within the region that is blue.*

Talairach coordinates for regions showing decreased perfusion in comparison of groups using t*-maps*

Group comparison	Region	Talairach coordinates
NC vs AC	Hippocampus (L)	−34, −16, −9
	Posterior cingulate (R)	15, −24, 46

Talairach coordinates for regions showing decreased perfusion in comparison of groups using t*-maps*

Group comparison	Region	Talairach coordinates
	Anterior cingulate (R)	9, 22, 36
	Anterior cingulate (L)	−12, 13, 36
	Posterior parietal lobe (L)	−32, −48, 37
	Superior frontal lobe (R)	21, −10, 55
	Superior frontal lobe (L)	−21, −10, 55
NC vs AD	Posterior parietal lobe (L)	−44, −65, 32
	Posterior parietal lobe (R)	44, −65, 32
	Superior frontal lobe (L)	−49, 38, 28
	Superior frontal lobe (R)	49, 38, 28
AC vs AD	Posterior parietal lobe (L)	−47, −66, 32
	Posterior parietal lobe (R)	47, −66, 32
	Superior frontal lobe (L)	−69, 34, 28
	Superior frontal lobe (R)	69, 34, 28
	Posterior	15, −24, 46

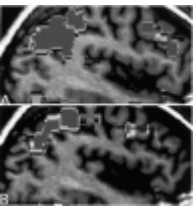

Talairach coordinates for regions showing decreased perfusion in comparison of groups using t*-maps*

Group comparison	Region	Talairach coordinates
	cingulate (R)	

NC = normal control noncarriers; AC = aymptomatic carriers of presenilin-1 gene (*PS-1*) mutation; AD = AD patients with *PS-1* mutation.

Figure 2. *This figure represents the region in the temporoparietal cortex (shown in color) that significantly differentiated the normal control noncarriers from the patients with AD (A) and the asymptomatic presenilin-1 gene mutation carriers from the patients with AD (B). (Note that the AD patients also differed from control subjects in the regions identified in figure 1 .) The SPECT data are overlaid on a typical MR image in sagittal section. The anatomic label assigned to the region is based on the examination of the t-map overlay on an average MR image obtained from 152 individuals.*[34] *The data were scaled to the Talairach coordinate system. The significant differences between the groups are highest within the region that is at the red end of the spectrum and lowest within the region that is blue.*

Vector analysis.

A discriminant function analysis was computed, using the weighted vector scores for the 20 vectors for each subject, covarying age and gender, to predict the group membership of the subjects in the three groups. The latter two variables were added to adjust for any possible differences between the groups based on these variables. This discriminant function was highly significant ($\chi^2 = 96.8$, $p < 0.0005$, canonical correlation = 0.92) and yielded one significant function. The overall accuracy of the discriminant function was 86%. It should be noted that the homogeneity of the group variances was examined and found to be satisfactory (ensuring that the small size of some of the groups did not compromise the analysis).

In addition, an algorithm based on the discriminant function from another study in which preclinical cases of AD were examined[17] was evaluated in the present sample. This algorithm, based on SVD, had utilized individuals in an ongoing longitudinal study related to predictors of the development of AD. It had successfully discriminated normal control subjects from individuals with memory problems who did not develop AD and from individuals with memory problems who subsequently progressed to meet criteria for AD within the follow-up period ($p < 0.0005$). When applied to the subjects in the current study, the algorithm was also highly statistically significant ($\chi^2 = 133.17$, $p < 0.00001$). Four of the vectors contributed to the discrimination between the groups in this study.

Correlation with neuropsychological measures.

Correlations were performed between the four vector scores that discriminated between the groups and the neuropsychological test performance of the participants in the study.

Each of the four vectors was significantly correlated with tests that assessed delayed recall of verbal and nonverbal information, confrontation naming, and figure copying. The significance of the correlations ranged from 0.01 to 0.0001.

Discussion.

The results indicate that asymptomatic carriers of the *PS-1* gene mutation have significant decreases in SPECT brain perfusion in comparison with normal control subjects before the time that they develop the clinical symptoms of AD. In addition, the differences in perfusion seen among individuals who are asymptomatic but are in the prodromal phase of the AD as a result of a mutation in the *PS-1* gene are similar to those seen in a previous study examining prodromal cases of AD not resulting from this gene mutation.[17] In both investigations, decreased SPECT perfusion was observed in the hippocampal complex and the anterior and posterior cingulate. The generality of these findings is also emphasized by the fact that the algorithm derived from the study of prodromal AD that did not include individuals with a *PS-1* mutation[17] significantly discriminated the subjects in the current study.

Moreover, in this study, the asymptomatic gene carriers also showed decreased perfusion in the posterior parietal lobe and the superior frontal lobe not seen in prodromal AD cases unrelated to this gene mutation. These latter abnormalities have, however, been reported in two PET studies[5] [6] that examined individuals at increased risk for late-onset AD because they carried either one or two alleles of the *APOE-4* gene, the gene that increases risk for AD among older individuals.

These data provide increasing evidence for the hypothesis that a network(s) of brain regions is altered in prodromal AD that includes the hippocampal complex and the posterior and anterior cingulate gyrus. Among individuals with a specific genetic risk for AD, cortical brain regions such as the posterior parietal lobe and superior frontal lobe also appear to demonstrate decreased perfusion.

Perfusion alterations in the hippocampal complex in prodromal AD are consistent with a large body of knowledge indicating that this region is involved at the earliest stage of this disorder.[35] [36] [37] Likewise, animal data suggest that the posterior cingulate together with the hippocampal formation make up a memory system critical for learning the relationships among cues, such as previously unrelated spatial or temporal features of the environment.[38] [39] The involvement of the anterior cingulate in prodromal AD has now been demonstrated in both functional and structural imaging studies[17] [40] and is hypothesized to be related to the executive function deficits seen early in the course of AD.[41] [42]

Decreased perfusion in the superior frontal cortex may also be related to the executive function deficits seen in prodromal AD, as this brain region is strongly and reciprocally connected with memory-related structures in the brain, including the entorhinal cortex and hippocampus.[43] [44] Perfusion defects in the parietal lobe are commonly described in established AD,[7] [8] [9] [10] [11] [12] and have been reported in at least one study of individuals at risk for AD.[6] However, the relationship of this abnormality to the functional deficits seen in prodromal AD is less clear because abnormalities in temporoparietal cortices

have not been associated with either memory or executive function deficits. Likewise, the neuropathologic changes associated with AD have not been reported to affect this cortical area at the earliest stage of AD. It has therefore been hypothesized that perfusion abnormalities are found in temporoparietal cortices because they contain distal projections of dendritic fields from the hippocampal complex.[45]

It is important to acknowledge the potential impact of age differences among the groups on the findings described above. Although the absolute difference in mean age between Groups 1 and 2 was only 4.6 years, this differential approached significance because of the extremely young age of all of the participants. The age difference between Groups 1 and 3 was 8.3 years, which was statistically significant. It was not possible to reduce the age difference among the groups by the elimination of the oldest participants because the analyses would have been jeopardized by a small sample size. Likewise, it was not possible to increase the sample size further because all available participants were studied and the Colombian kindred as a whole is a rare and unique resource. It nevertheless seems unlikely that the results described above are an artifact of these age differences. In a previous study using SPECT, employing similar analytic techniques,[20] it was reported that age-related differences are primarily reflected by decreased uptake in the lateral ventricles. In the same study, it was also found that females had increased (rather than decreased) perfusion in selected brain regions compared with males, suggesting that any differences in the number of males and females between the groups also could not account for the declines in perfusion observed in Groups 2 and 3 in comparison with Group 1.

It should also be noted that the identification of the regions with decreased perfusion in the current study could be due to the combined effects of atrophic change and decreased perfusion on the data because the scaling method employed mitigated, but could not eliminate, alterations secondary to brain shrinkage. However, even if the data combine information about both perfusion and underlying brain volume, the importance of the findings lies in the early detection of the changes and in the regional distribution of the brain regions that contribute to the discrimination.

The data therefore suggest that regional cerebral perfusion abnormalities based on SPECT are detectable before development of the clinical symptoms of AD in carriers of the *PS-1* mutation. Further evaluation of these subjects may demonstrate how such abnormalities evolve over time with the expression of this gene mutation.

References

1. Cruts M, van Duijn C, Backhovens H, et al. Estimation of the genetic contribution of presenilin 1 and 2 mutations in a population-based study of presenilin Alzheimer disease. Hum Mol Genet 1998;7:43–51. Abstract

2. Lopera F, Ardilla A, Martinez A, et al. Clinical features of early-onset Alzheimer disease in a large kindred with E280A presenilin-1 mutation. JAMA 1997;12:793–799. Abstract

3. Freeborough P, Fox N. MR image texture analysis applied to the diagnosis and tracking of Alzheimer's disease. IEEE Trans Med Imag 1998;17:475–479.

4. Saunders A, Strittmatter W, Schmechel D, et al. Association of apolipoprotein E allele e4 with late

onset familial and sporadic Alzheimer's disease. Neurology 1993;43:1467–1472. Abstract

5. Reiman E, Caselli R, Yun L, et al. Preclinical evidence of Alzheimer's disease in persons homozygous for the epsilon 4 allele for apolipoprotein E. N Engl J Med 1996;334:752–758. Abstract

6. Small G, Mazziotta J, Collins M, et al. Apolipoprotein E type 4 allele and cerebral glucose metabolism in relatives at risk for familial Alzheimer disease. JAMA 1995;273:942–947. Abstract

7. Farkas T, Ferris SH, Wolf AP, et al. ^{18}F-2-Deoxy-2-fluoro-D-glucose as a tracer in the positron emission tomographic study of senile dementia. Am J Psychiatry 1982;139:352–353. Citation

8. Friedland R, Budinger T, Ganz E, et al. Regional cerebral metabolic alterations in dementia of the Alzheimer type: positron emission tomography with [^{18}F]fluorodeoxyglucose. J Comput Assist Tomogr 1983;7:590–598. Abstract

9. Foster N, Chase T, Mansi L, et al. Cortical abnormalities in Alzheimer's disease. Ann Neurol 1984;16:649–654. Abstract

10. Duara R, Grady C, Haxby J, et al. Positron emission tomography in Alzheimer's disease. Neurology 1986;36:879–887. Abstract

11. Holman BL, Johnson K, Gerada B, et al. The scintigraphic appearance of Alzheimer's disease: a prospective study using technetium-99m-HMPAO SPECT. J Nucl Med 1992;33:181–185. Abstract

12. Johnson K, Kijewski M, Becker J, et al. Quantitative brain SPECT in Alzheimer's disease and normal aging. J Nucl Med 1993;34:2044–2048. Abstract

13. DeKosky S, Shih W-J, Schmitt F, et al. Assessing utility of single photon emission computed tomography (SPECT) scan in Alzheimer disease: correlation with cognitive severity. Alzheimer Dis 1990;4:14–23.

14. McGeer E, McGeer P, Harrop R, et al. Correlations of regional postmortem enzyme activities with premortem local glucose metabolic rates in Alzheimer's disease. J Neurosci Res 1990;27:612–619. Abstract

15. Smith G, de Leon M, George A, et al. Topography of cross-sectional and longitudinal glucose metabolic deficits in Alzheimer's disease. Pathophysiologic implications. Arch Neurol 1992;49:1142–1150. Abstract

16. Jobst K, Barneston L, Shepstone B. Accurate prediction of histologically confirmed Alzheimer's disease and the differential diagnosis of dementia: the use of NINCDS-ADRDA and DSM III-R criteria, SPECT, x-ray CT and APOE4 medial temporal lobe dementias. Int Psychogeriatr 1997;9:191–222. Abstract

17. Johnson K, Jones K, Becker J, et al. Preclinical prediction of Alzheimer's disease using SPECT. Neurology 1998;50:1563–1571. Full Text

18. Folstein M, Folstein S, McHugh P. “Mini-Mental State.” A practical method for grading the cognitive state of patients for the clinician. J Psychiatr Res 1975;12:189–198. Citation

19. McKhann G, Drachman D, Folstein MF, et al. Clinical diagnosis of Alzheimer's disease: report of the NINCDS-ADRDA Work Group under the auspices of Department of Health and Human Services Task Force. Neurology 1984;34:939–944. Abstract

20. Jones K, Johnson K, Becker J, et al. Use of singular value decomposition to characterize age and gender differences in SPECT cerebral perfusion. J Nucl Med 1998;39:965–973. Abstract

21. Morris J, Heyman A, Mohs R, et al. The Consortium to Establish a Registry for Alzheimer's Disease (CERAD). Neurology 1989;39:1159–1165. Abstract

22. Kaplan E, Goodglass H, Weintraub S. Boston Naming Test. Philadelphia: Lea & Febiger, 1978.

23. Goodglass H, Kaplan E. Assessment of aphasia and related disorders. Philadelphia: Lea & Febiger, 1972.

24. Rey A. L'examen psychologique dans les cas d'encephalopathie traumatique. Arch Psychol 1941;28:286–340.

25. Wechsler D. The Wechsler Adult Intelligence Scale–revised. New York: Psychological Corp., 1988.

26. Wechsler D. A standardized memory scale for clinical use. J Psychol 1945;19:87–95.

27. Genna S, Smith A. The development of ASPECT, an annular single crystal brain camera for high efficiency SPECT. IEEE Trans Nucl Sci 1988;35:654–658.

28. Holman BL, Carvallo P, Zimmerman R, et al. Brain perfusion experience. J Nucl Med 1990;31:654–658. Abstract

29. Talairach J, Tournoux P. Co-planar stereotaxic atlas of the human brain. New York: Thieme Medical, 1988.

30. Friston K, Frith C, Liddle P, et al. The relationship between global and local changes in PET scans. J Cereb Blood Flow Metab 1990;10:458–466. Abstract

31. Ford I, McColl J, McCormack A, et al. Statistical issues in the analysis of neuroimages. J Cereb Blood Flow Metab 1991;11:A89–A95. Abstract

32. Ford I. Some nonontological and functionally unconnected views on current issues in the analysis of PET datasets. J Cereb Blood Flow Metab 1995;15:371–377. Abstract

33. Friston K. Statistical parametric mapping. Ontology and current issues. J Cereb Blood Flow Metab 1995;15:361–370. Citation

34. Collins DL, Neelin P, Peters TM, Evans AC. Automatic 3D intersubject registration of MR volumetric data in standardized Talairach space. J Comput Assist Tomogr 1994;18:192–205. Abstract

35. Ball MJ. Neuronal loss, neurofibrillary tangles and granulovacuolar degeneration in the hippocampus with ageing and dementia. A quantitative study. Acta Neuropathol 1977;37:111–118. Abstract

36. Hyman B, Van Hoesen G, Kromer C, et al. Alzheimer's disease: cell specific pathology isolates the hippocampal formation. Science 1984;225:1168–1170. Abstract

37. Gómez-Isla T, Price JL, McKeel DW, et al. Profound loss of layer II entorhinal cortex neurons occurs in very mild Alzheimer's disease. J Neurosci 1996;16:4491–4500. Abstract

38. Sutherland R, Rudy J. Configurational association theory: the role of the hippocampal formation in learning, memory and amnesia. Psychobiology 1989;17:129–144.

39. Sutherland R, Rudy J. Exceptions to the rule of space. Hippocampus 1991;1:250–252. Citation

40. Killiany R, Gomez-Isla T, Moss M, et al. Use of structural MRI to predict who will get Alzheimer's disease. Ann Neurol 2000;47:430–439. Abstract

41. Lafleche G, Albert M. Executive function deficits in mild Alzheimer's disease. Neuropsychology 1995;9:313–320.

42. Albert M, Moss M, Tanzi R, et al. Preclinical prediction of AD using neuropsychological tests. JINS (in press).

43. Vogt B, Crino P, Volicer L. Laminar alterations in gamma-aminobutyric acid-A, muscarinic, and beta adrenoceptors and neuron degeneration in cingulate cortex in Alzheimer's disease. J Neurochem 1991;57:282–290. Abstract

44. Van Hoesen G, Solodkin A. Some modular features of temporal cortex in humans as revealed by pathological changes in Alzheimer's disease. Cereb Cortex 1993;3:465–475. Abstract

45. Meguro K, Blaizot X, Kondoh Y, et al. Neocortical and hippocampal glucose metabolism following neurotoxic lesions of the entorhinal and perirhinal cortices in the non-human primate. Brain 1999;2:1519–1531. Abstract

Find Similar Articles